

HOSTED BY



ELSEVIER

Available online at [www.sciencedirect.com](http://www.sciencedirect.com)

ScienceDirect

journal homepage: <http://www.elsevier.com/locate/jsm>

# Geomechanical conditions of causes of high-energy rock mass tremors determined based on the analysis of parameters of focal mechanisms



Krystyna Stec\*

Department of Geology and Geophysics, Central Mining Institute, Katowice, Poland

## ARTICLE INFO

## Article history:

Available online 2 September 2015

## Keywords:

Rock mass tremor  
Focal mechanism  
Principal stresses

## ABSTRACT

The aim of the research was to determine the cause of high-energy rock mass tremors (energy  $E \geq 10^5$  J) in the area of longwall H-2a located in seam 409/3 in Borynia-Zofiówka-Jastrzębie colliery, basing on the analysis of geological and mining conditions, seismic activity, focal mechanism and local stress field. The research employed the method of seismic moment tensor inversion which provides parameters of focal mechanism (percentage share of its components: isotropic, uniaxial compression or tension, shear component; trend and dip of nodal planes, directions of tension axes and compression stress). The parameters describe processes occurring in focuses of tremors and they are clearly linked with stress conditions in a given area. The conducted tests showed that the cause of occurrence of high-energy tremors and three rockbursts in lot H while mining seam 409/3 with longwall H-2a, was dynamic destruction of roof rocks which could displace towards the cavity created after mining the seam. An additional factor significantly magnifying the process was the share of stresses, which originate from the faults in the area, existing in the rock mass. Results of the research provided additional information to determine the degree of rockburst hazard in the area. Because of very dangerous work conditions (stress parameters reflect the rock mass of high shear strength, where dynamic influence of tremors is stronger) mining activity in longwall H-2a was terminated a few dozen metres earlier than it had been originally planned.

© 2015 The Author. Production and hosting by Elsevier B.V. on behalf of Central Mining Institute in Katowice. This is an open access article under the CC BY-NC-ND license (<http://creativecommons.org/licenses/by-nc-nd/4.0/>).

## 1. Introduction

Underground mining of coal deposits disturbs equilibrium of a system of natural stresses in the rock mass, both in direct vicinity and further away from mine workings. The process results in, among others, rock mass tremors, which in some

cases are a direct cause of rockbursts. The phenomenon of rockburst, due to its dynamic character, causes certain effects in workings within its range. These may be accidents of the personnel and material loss in form of destroyed or damaged machines, equipment and workings losing their functionality. Unfortunately, these are often incidents of a mining catastrophe scale i.e. a group accident with casualties and seriously

\* Tel.: +48 32 259 23 38.

E-mail address: [kstec@gig.eu](mailto:kstec@gig.eu).

Peer review under responsibility of Central Mining Institute in Katowice.

<http://dx.doi.org/10.1016/j.jsm.2015.08.008>

2300-3960/© 2015 The Author. Production and hosting by Elsevier B.V. on behalf of Central Mining Institute in Katowice. This is an open access article under the CC BY-NC-ND license (<http://creativecommons.org/licenses/by-nc-nd/4.0/>).

wounded personnel. That is why research works on developing more efficient preventive measures, which would reduce the threat, are conducted in many research centres in Poland and around the world. Seismic phenomena and rockburst hazard associated with it in a given longwall panel are influenced by a number of natural and technical factors. The dominant ones are strength parameters of coal and surrounding rocks, and the volume of stresses in the vicinity of operating workings (Bukowska, 2013; Dubiński, 2013). As it is known the source of high-energy mining tremors are fracturing layers of high strength rock mass (Drzewiecki & Kabiesz, 2008). The process of fracturing rocks in a focus can be determined basing on parameters describing the focal mechanism of tremors. The parameters are calculated with seismic moment tensor inversion basing on the analysis of seismic waves generated in a tremor focus and recorded by sufficient number of seismometers located around the focus. Parameters of a focal mechanism are fundamental for determining a relative local stress field described with the direction of principal stresses and their mutual relations, which in turn enable evaluating stress state of the rock mass of higher or lower tendency to generate high-energy tremors. It ought to be noted that the spatial system of principal stresses axes determines occurrence of tremors of various focal mechanism (Stec, 2012). Of course, basing only on seismologic data, it is impossible to determine absolute values of stress. Yet, it is possible to determine their spatial orientation and mutual relations. It turns out that tremors of different focal mechanisms, i.e. with different spatial seismic influence, can have a different influence on the process of destroying the structure of rock mass and losing stability in the already existing, or just forming, planes of weakening. Hence an analysis of focal mechanism tremors, especially high-energy seismic phenomena, started to play an important role in determining causes and occurrence of tremors, and for rockbursts, which caused damage to the mine workings, it became a standard procedure (Stec & Drzewiecki, 2012). Calculations of focal mechanism parameters, and according to them local stress field were conducted for high-energy rock mass tremors which accompanied mining seam 409/3 with longwall H-2a in Zofiówka colliery.

## 2. Characteristics of the tested area

The tested area covered longwall H-2a, seam 409/3, lot H, of Zofiówka colliery. Seam 409/3 occurring within a group of seams 409 in the monoclonal part of the seam, of approximately  $10^\circ$  eastward dip, has a complicated structure. Eastward and southward its thickness increases from approximately 1.6 to 2.6 m, and in the southern part of the discussed area a 0.80 m layer of coal gets separated from its top (distance 0.3–1.0 m). Seam 409/3 in the area of longwall H-2a occurs at the depth of between 840 m and 950 m. In the eastern part of lot H there is the “eastern” fault of N–S strike and eastward drop  $h = 25\text{--}15$  m; the western border of the lot is Jastrzębie fault, also of N–S strike and westward drop  $h = 25\text{--}50$  m (Fig. 1). The disturbances are accompanied by parallel faults of drop of up to 3 m. Normal fault of drop of approximately 5 m runs, roughly W–E, through the central part

of lot H. Geological structure of the rock mass, both above and below seam 409/3, shows diversified lithology. In the roof of the seam there are: sandy mudstone, locally with single laminae of coal (0.0–0.90 m), siltstones (0.0–2.25 m). Then there is sandstone, with intercalations of siltstone (12.0–41.0 m) of  $R_c = 61\text{--}106$  MPa, locally in the immediate roof strata of the seam. Above there is siltstone, with intercalations of fine-grained sandstone ( $\sim 0.0\text{--}15.0$  m), mudstone with laminae of coal (0.0–2.70 m), and seam 409/2 ( $\sim 0.78\text{--}0.85$  m). Over seam 409/2 there is siltstone, with local laminae of mudstone (0.0–4.0 m), and then a layer of thick-bedded sandstone of thickness between 15.0 m and 22.1 m. Floor layers of seam 409/3 also show geological diversification. In the floor of the seam there are: mudstone with thick laminae and layers of coal, locally of coal shale characteristics (0.50–1.30 m), and seam 409/4 of thickness of 4.2–5.2 m. In the area of longwall H-2a there are four edges of previous mining activities i.e. seam 408/2 at the distance of 64–73 m, seam 406/1 at the distance of 173–198 m, seam 404/4 at the distance of 223–251 m, and seam 409/4 at the distance of 0.4–20 m (Fig. 1). Seam 409/3 in lot H is ranked as: III degree rockburst hazard, I degree water hazard, IV category methane hazard, class B coal dust explosion hazard, and methane-and-rock outburst hazard.

Exploitation of longwall H-2a, with roof cave-in from east westward up the rise of seam, started on 10 June 2013. Because of potentially high seismic hazard in the area (III degree of rockburst hazard) torpedo blasting of the roof of seam 409/3 from the gateroads was conducted within the framework of active rockburst prevention. Zones of particularly high rockburst hazard were determined in tailgate H-2, where slim holes were drilled two times a week. There were also three series of seismic measurement (geotomography). The basic goal of geophysical interpretation of underground seismic measurement results is to determine the distribution of seismic wave propagation velocity in the medium being (coal seam or adjacent strata) that could reveal its structural features or their changes. The criteria characterising the anomalies of seismic P-wave propagation velocity have been implemented by Dubiński and Dworak (1989). The obtained values of a seismic anomaly showed influence of the edge of seams 408/2 and 406/1, and average increase in stress in the longwall lot.

Since the very beginning of the mining activity in the area there has been seismic activity which caused high rockburst hazard. While operating longwall H-2a and driving a recovery room for the powered roof support sections 99 tremors of energy of  $10^2$  J, 360 tremors of energy of  $10^3$  J, 84 tremors of energy of  $10^4$  J, 13 tremors of energy of  $10^5$  J and 4 tremors of energy of  $10^6$  J were recorded. There were three tremors among them which resulted in certain effects in the workings. On 6 November 2013 there was a rock mass tremor of energy of  $E = 4.6 \cdot 10^6$  J, located in longwall gobs. The tremor caused distressing the rock mass in tailgate H-2 of seam 409/3, and exceeding the acceptable concentration of methane in the sensors installed in the area. There was damage to the gateroads (floor heave) and the gateroad support. After the tremor, mining activities were paused until 20 December 2013 when they were resumed. Yet, on 30 January 2014 there was another rock mass tremor of energy of  $E = 3.7 \cdot 10^6$  J, located along the face of longwall H-2a, which caused separation of sidewalls and damaged several

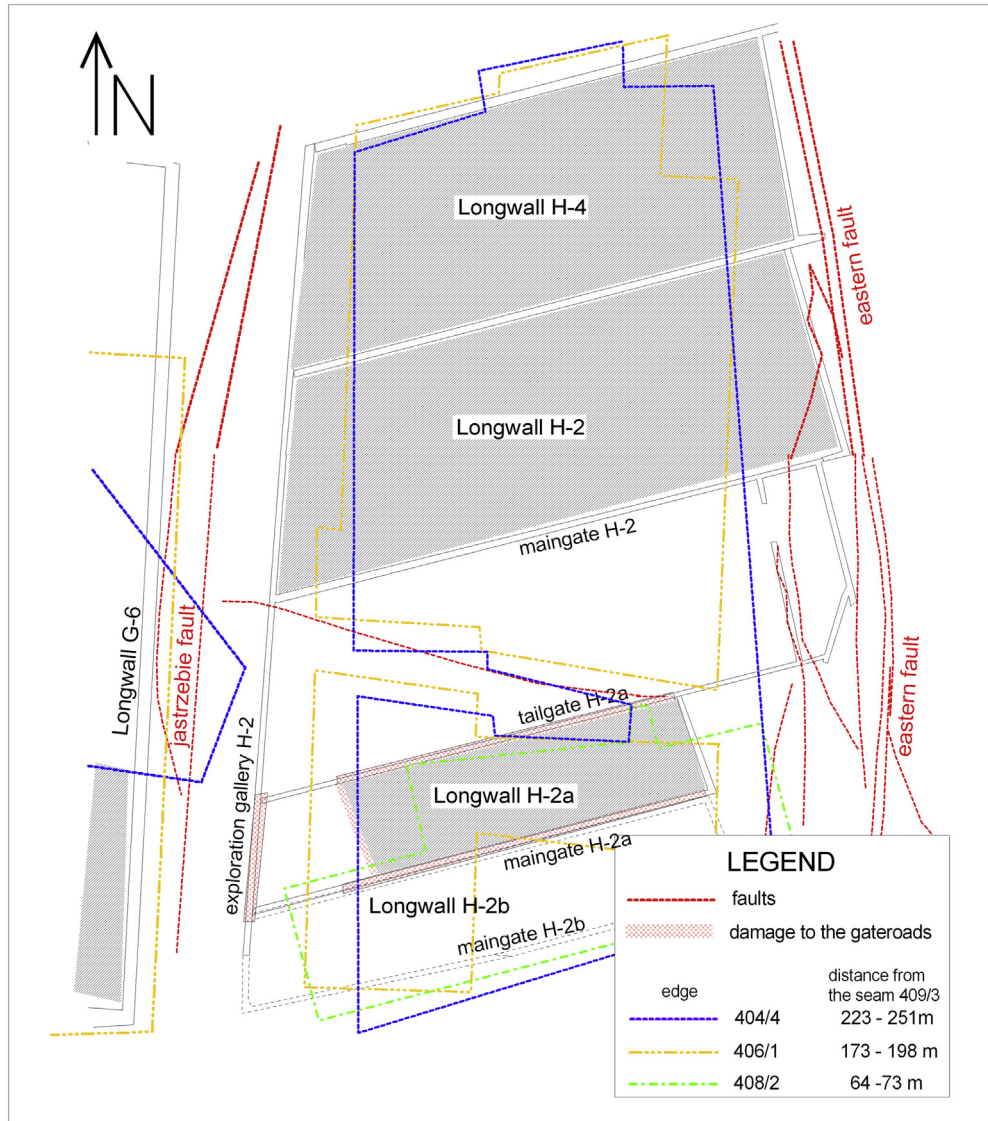


Fig. 1 – Fragment of the map of seam 409/3 lot H.

sections of the powered roof support. Because of high rockburst hazard in the area the Department of Rockburst and Roof Fall Hazard accompanied by specialists from other academic institutions, decided, basing on the results of the tests, to finish mining activities in longwall H-2a at that stage. Then recovery works were carried out (disassembly of the shearer and the conveyors) and driving gateroads for the next designed longwall H-2b started. On 19 June 2014 at 6:39:10 there was a rock mass tremor of very high energy of  $2 \cdot 10^8$  J, which was located approximately 50 m ahead of recovery room of the powered roof support sections in longwall H-2a and approximately 20 m north of tailgate H-2a in the area of the edge of former mining activities in seams 408/2 and 406/1. After the tremor, 48 s later an aftershock of energy of  $E = 5.1 \cdot 10^5$  J came, located in the same area. As a consequence of the phenomena there was floor heave of total length of approximately 80 m in gateroads (exploration gallery H-2, tailgate H-2, tailgate H-2a, maingate H-2b). The

support was deformed and broken, and the roof caved in. The tremor also disturbed ventilation parameters and caused exceeding acceptable concentrations of methane. In the area, at that time, the mining works were not advanced and nothing indicated a possibility of occurrence of a tremor of such high energy. Only the following mining works were conducted:

- driving maingate H-2b in seam 409/3 – horizontal distance of approximately 90 m from the focus of the tremor of energy of  $2 \cdot 10^8$  J,
- driving tailgate H-2b w seam 409/3 – horizontal distance of approximately 200 m from the focus of the tremor of energy of  $2 \cdot 10^8$  J,
- in lot G, west of Jastrzebie fault, seams 412lg+ld and 412lg were mined with longwall G-6 – horizontal distance of approximately 240 m from the focus of the tremor of energy of  $2 \cdot 10^8$  J.

### 3. Results of calculations of focal mechanism of tremors in longwall H-2a

While mining seam 409/3 with longwall H-2a, there were high-energy tremors of energy of  $E \geq 1.0 \cdot 10^5$  J and during recovery works conducted in longwall H-2a there was a tremor of energy of  $2.0 \cdot 10^8$  J. For 25 tremors of the highest energy the focal mechanism was calculated with seismic moment tensor inversion method. The moment tensor inversion method was based on the software FOCI developed by Kwiatek ([www.induced.pl](http://www.induced.pl)) in the Institute of Geophysics of the Polish Academy of Sciences. The input parameters were the amplitude and polarity information on the first P-wave displacement pulses.

As a result of the calculations with use of mentioned above FOCI software, three solutions were obtained for each event:

- The full moment tensor, which can be decomposed into an isotropic component (ISO) describing the volume change: explosion  $+/+$  or implosion  $-/-$ , and into a compensated linear vector dipole (CLVD) corresponding to the uniaxial compression  $-/-$  or tension  $+/+$ , and into the double-couple component (DC) corresponding to the shear motion.
- The deviatoric tensor which has a CLVD component and the shear component DC.
- Pure shear tensor, having only the double-couple (DC) component.

The full, deviatoric, and pure shear moment tensor were calculated using the L1 norm as a measure of the misfit and the method of the Lagrange multipliers (Gibowicz & Kijko, 1994; Wiejacz, 1991). The accuracy of focal mechanism determination was controlled using the solution quality factor Q which ranges from 0 to 100% and chosen for the lowest uncertainty ERR. The quality of the solution differed due to numerical errors of solution and compatibility of direction of first arrival signs of the P wave. The results for  $Q < 40\%$  have been discarded.

The calculation were based on seismograms recorded by seismic network at the Borynia-Zofiówka-Jastrzębie Ruch Zofiówka colliery. During the research the seismic network is composed of 32 vertical Wilmore seismometers are located underground at the level of coal seams. The recording stations were horizontally and vertically spaced from the epicentral area at distances ranging from 300 to 6000 m and from 200 to 800 m, respectively. Fig. 2 shows the spatial distribution the seismic station and the seismic events incorporated in moment tensor inversion calculations. For analysis were taken only the nearest stations in which were the first P-wave displacement pulses explicit (number of stations used in focal mechanism are shown in Table 1).

The accuracy of a focal model to a large extent depends on accurately determined tremor focus. The events, located by the mine's staff with MULTILOK software exhibit uncertainties in the epicentral coordinates of the order of  $\pm 50$  m, which are much smaller than the uncertainty in depth determination equal over 100 m (Lurka & Logiewa, 2007). This is because of the location of seismometers mainly at the level of coal seams. The MULTILOK software for tremor location is

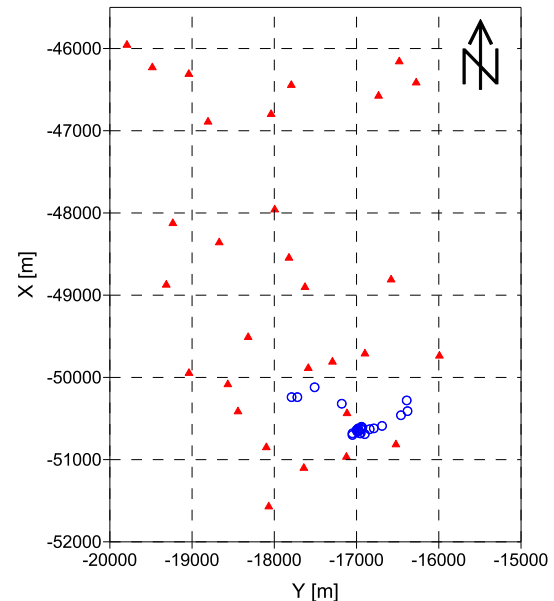












Fig. 2 – Spatial distribution of the analysed events (blue circles) along with the seismic stations (triangles).

able to select one of the following minimization algorithms: Simplex, modified Powell algorithm, and the Davidson-Fletcher-Powell algorithm (Lurka, 1996). This software used for the location of mining tremor foci and seismic energy determination in Upper Silesia has a positive opinion of the State Mining Authority (WUG) no. GEM/422/0016/00/03943/AR of 9 May 2000.










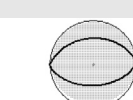

In this analysis, the depth of focus of analysed tremors was computed with use of the moment tensor inversion method, based on the best fit of the solution, chosen for the lowest uncertainty ERR and the highest quality factor Q (parameters ERR and Q computed by using the options in the FOCI software). Results of calculations of mentioned coefficients showed that the focuses of the analysed tremors could occur at the depth of between  $-550$  m BSL and  $-700$  m BSL, except for one tremor of 19 June 2014 of energy of  $2 \cdot 10^8$  J, the depth of the tremor was  $-400$  m BSL (error in calculation of focus depth was  $\pm 20$  m). Table 1 gives information on the fault plane solutions. It is a solution of full tensor, where distinguished: isotropic component (ISO), Compensated Linear Vector Dipole (CLVD) and shear component (DC). Distribution of tremors on the map together with a diagram of a focal mechanism are presented in Fig. 2. A diagram of a focal mechanism shows the lower hemisphere. The obtained solutions of focal mechanisms provide information on the share of the above mentioned components in a process of tremor occurrence. An explosive or implosive focus model reflects the processes of volumetric destruction of the medium structure (e.g. tremors occurring after shock blasting or within a seam). Compensated linear vector dipole reflects roughly uniaxial compression or tension. The model was used in describing sudden phase transformations in focuses of deep earthquakes, ruptures of rocks are associated with tension in the presence of high-pressure liquids and mining tremors in the area of protective pillars in deep gold- and copper-mines. In turn the mechanism, where shear processes dominate in a plane

**Table 1 – Parameters of focal mechanism of tremors of energy of  $E \geq 1.010^5$  J occurring during while mining longwall H-2a, seam 409/3, Borynia-Zofiówka-Jastrzębie colliery. Denotations:  $\Phi_{A,B}$  – nodal plane trend A,B;  $\delta_{A,B}$  – dip of plane A,B;  $\lambda$  – slip angle;  $\Phi_{P,T}$  – axis trend P,T;  $\delta_{P,T}$  – plunge of axis P,T; ISO – percentage of isotropic component, explosion /+ or implosion /- /; CLVD – percentage of compensated linear vector dipole component, compression /- / or tension /+ /; DC – percentage of shear component (double-couple); NO – normal fault; RE – reverse fault; EXP – non-shear mechanism;  $Q_F$  – quality factor for full tensor;  $Q_D$  – quality factor for deviatoric tensor;  $Q_S$  – quality factor for pure shear tensor.**

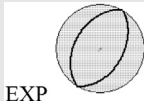




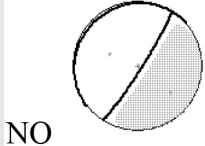
No Date (yyyy-mm-dd) Time (CET)	Energy [J]	Number of station	H [m BSL] error $\pm 20$ m	ISO CLVD DC [%]	Nodal plane		Axis		Focal mechanism 	$Q_F$ $Q_D$ $Q_S$ [%]
					A	B	P	T		
					$\Phi$	$\Phi$	$\Phi$	$\Phi$		
					$\Delta$	$\Delta$	$\Delta$	$\Delta$		
				$\lambda$	$\lambda$	$[\circ]$	$[\circ]$			
1. 2011-02-10 11:42:59	3.910 <sup>6</sup>	18	-700	23	24	152	316	100		43
				4	76	22	56	29		45
				73	-73	-140				33
2. 2012-02-05 7:35:48	8.210 <sup>5</sup>	18	-620	-7	36	196	309	123		70
				-7	82	8	53	37		74
				86	-87	-109				55
3. 2012-12-13 20:00:36	4.310 <sup>6</sup>	22	-620	-12	242	77	149	334		68
				-12	82	9	54	36		71
				76	88	105				53
4. 2013-07-28 22:20:42	1.610 <sup>5</sup>	12	-640	-19	156	342	29	249		50
				-20	49	42	86	3		55
				61	-94	-86				43
5. 2013-09-01 22:23:40	1.610 <sup>5</sup>	12	-600	-18	53	217	341	137		45
				-19	62	29	72	17		47
				63	-82	-104				39
6. 2013-09-22 22:07:04	1.310 <sup>5</sup>	12	-570	-13	198	49	101	293		46
				-20	80	11	54	35		51
				67	84	121				40
7. 2013-10-20 21:28:55	1.210 <sup>5</sup>	12	-600	-20	23	206	236	115		45
				-20	46	44	89	1		46
				60	-91	-89				38
8. 2013-10-29 4:35:15	1.810 <sup>5</sup>	12	-590	-20	149	321	96	236		46
				-20	50	40	84	5		48
				60	95	84				40
9. 2013-10-30 21:29:29	4.010 <sup>5</sup>	14	-640	-20	335	148	301	62		53
				-20	47	43	87	2		53
				60	94	86				41

(continued on next page)

Table 1 – (continued)

No Date (yyyy-mm-dd) Time (CET)	Energy [J]	Number of station	H [m BSL] error $\pm 20$ m	ISO CLVD DC [%]	Nodal plane		Axis		Focal mechanism 	Q <sub>F</sub> Q <sub>D</sub> Q <sub>S</sub> [%]
					A	B	P	T		
					$\Phi$	$\Phi$	$\Phi$	$\Phi$		
					$\Delta$ $\lambda$ [°]	$\Delta$ $\lambda$ [°]	$\Delta$ $\lambda$ [°]	$\Delta$ $\lambda$ [°]		
10. 2013-11-03 11:22:39	1.110 <sup>5</sup>	14	-560	-20 -19 61	13 51 -98	206 39 -80	242 81 109	6		53 56 44
11. 2013-11-04 22:40:59	3.610 <sup>5</sup>	12	-520	-14 -5 81	353 65 -94	183 26 -81	254 70 86	20		49 49 37
12. 2013-11-06 12:22:52	4.610 <sup>6</sup>	20	-550	1 6 93	41 82 94	197 9 67	128 37 315	53		62 65 48
13. 2013-12-29 22:47:04	1.310 <sup>6</sup>	20	-610	-10 -20 70	238 48 -87	53 43 -94	191 87 326	2		65 63 47
14. 2014-01-09 10:17:19	1.810 <sup>6</sup>	20	-580	-20 -20 60	23 48 -90	203 42 -90	294 87 113	3		68 68 51
15. 2014-01-23 15:43:34	7.810 <sup>5</sup>	18	-580	-24 -25 51	63 54 -60	199 46 -124	33 66 133	4		50 27 21
16. 2014-01-26 21:01:26	1.810 <sup>6</sup>	20	-580	48 48 4						56 59 46
17. 2014-01-30 18:21:01	3.710 <sup>6</sup>	22	-600	43 42 15	160 62 94	332 28 83	248 17 80	73		62 65 50
18. 2014-02-01 16:20:11	1.810 <sup>5</sup>	12	-550	49 49 2						36 42 36
19. 2014-02-05 18:15:43	1.210 <sup>5</sup>	12	-600	42 40 18						38 40 26

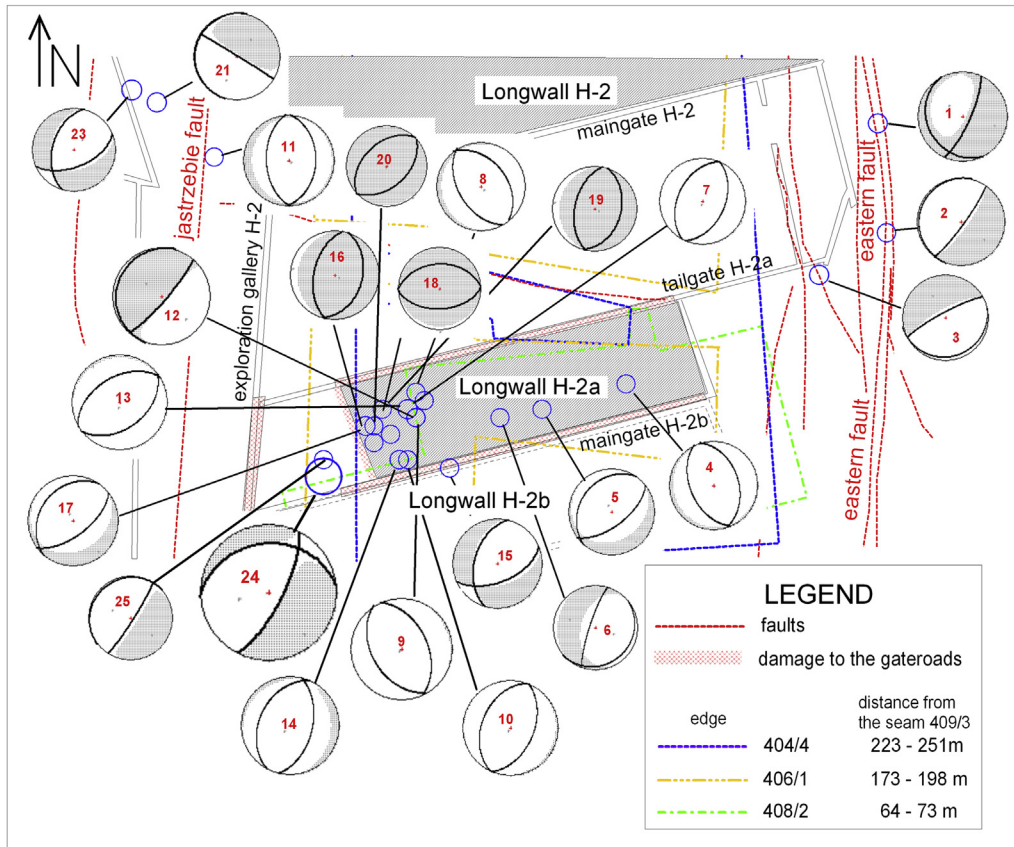
**Table 1 – (continued)**

No Date (yyyy-mm-dd) Time (CET)	Energy [J]	Number of station	H [m BSL] error $\pm 20m$	ISO CLVD DC [%]	Nodal plane		Axis		Focal mechanism	Q <sub>F</sub> Q <sub>D</sub> Q <sub>S</sub> [%]
					A	B	P	T		
					$\Phi$	$\Phi$	$\Phi$	$\Phi$		
					$\Delta$	$\Delta$	$\Delta$	$\Delta$		
$\lambda$	$\lambda$	[°]	[°]	[°]	[°]					
20. 2014-02-17 11:26:50	1.810 <sup>5</sup>	12	-600	58 37 5						48 42 18
21. 2014-04-02 17:30:45	5.310 <sup>5</sup>	16	-570	-27 -13 60	311 78 -96	156 14 -65	213 57 32	46		58 62 47
22. 2014-06-04 8:51:10	4.910 <sup>5</sup>	14	-550	-18 -12 70	344 75 -91	168 14 -86	253 59 31	75		49 51 39
23. 2014-06-13 21:12:58	2.710 <sup>5</sup>	12	-500	-17 -17 66	182 64 -119	55 38 -44	49 60 14	293		42 31 24
24. 2014-06-19 06:39:10	2.010 <sup>8</sup>	32	-400	-0.3 7 93.7	27 73 -115	265 30 -36	266 55 24	136		85 69 51
25. 2014-06-19 06:39:58	5.110 <sup>5</sup>	16	-580	-15 -9 76	32 84 -92	230 6 -73	300 51 39	124		50 54 45

described with a double pair of forces, reflects tremors associated with roof rocks fracturing or tremors occurring in fault zones.

As it can be seen in Table 1, focal mechanism in which shear processes dominated – normal slip focal type was obtained for most of the analysed tremors. Because of diverse trends of nodal planes, it was not possible to choose a dominant direction of fracturing in the focus of all the tremors (Fig. 3). For several tremors a plane of roughly NE-SW trend, and for the rest of them of roughly NNW-SSE or E-W strike were selected as the fracturing plane. For the full seismic moment tensor in the focuses of tremors the proportions were: between 60% and 94% of shear component, between approximately 5% and 23% of isotropic component, and between 5% and 20% of uniaxial compression component. Because the analysed area is surrounded by fault zones we cannot exclude that the tectonic structures influence the way the rock mass is destroyed. Longwall H-2a is located in a goaf zone – both east and west of

it there are normal faults, which dip their layers eastward and westward i.e. in two opposite directions. Hence, it may be assumed, that in the area the influence of stress originating in the fault structures, with high probability, is reflected by tremors, for which direction of the trend of one of the nodal planes can be correlated with the strike of the fault zone and the focuses were characterized by a very high share of the shear component of over 70%. The selected nodal planes also had dip of over 70°. It may be then concluded that the tremors of that mechanism could be a result of processes of fracturing which occurs in the roof layers as a consequence of simultaneous influence of mining stresses and stresses associated with the influence of fault zones. The tremor of 19 June 2014 of very high energy of  $E = 2 \cdot 10^8$  J confirms existence of significant stresses in the area, which were already detected with geo-mechanical tests (Documentation GIG no. 581 4793 3-141, 2013). The tremor occurred after operations in longwall H-2a stopped. As it was specified in the previous section of the paper



**Fig. 3 – Location and focal mechanism of high-energy tremors in the area of longwall H-2a, seam 409/3, Borynia-Zofiówka-Jastrzębie colliery.**

it damaged workings of total length of 80 m. The tremor was also detected on the surface within the range of a few kilometres. The origin of the type of high-energy phenomena was explained basing on geomechanical analyses conducted in previous years. According to Drzewiecki and Makówka (2013) tremors of that type can be a result of fracturing rock layers, which gained ability to displace towards the cavity created after mining a seam. The roof layers displace towards it, deflect over goafs and they can undergo dynamic destruction. An additional factor, in the analysed area of longwall H-2a, which significantly magnifies the process, was the share of stresses already existing in the rock mass, which originated from the faults in the area.

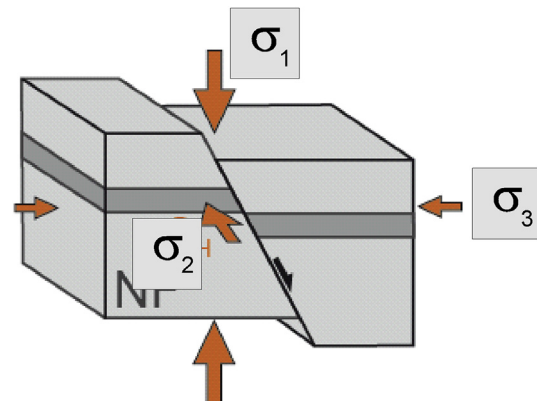
For the other tremors of shear mechanism, strike trend of one of nodal planes (NNW-SSE) can be correlated, within measurement error (20°), with the strike of the longwall face. Taking into consideration the type of focal mechanism of the tremors (normal slip), their depth (–550– –640 m BSL) and the direction of fracturing within the focus, which was parallel to the longwall face, it can be concluded that they were caused by the processes of fracturing and imploding of roof layers subject to tremors occurring as a consequence of the increasing longwall advance.

A few phenomena were characterised by a mechanism of large percentage share of non-shear processes. Explosive and CLVD components were over 40%. Tremors of the mechanism occurred after the actions aimed at destressing a given section

of rock mass. The active rockburst prevention included torpedo blasting in the gateroads.

**4. Characteristics of the local stress field in the area of longwall H-2a**

Parameters of focal mechanism expressed with trend and dip of nodal planes, and slip angle can be used in determining relative local stress field, described with distribution of

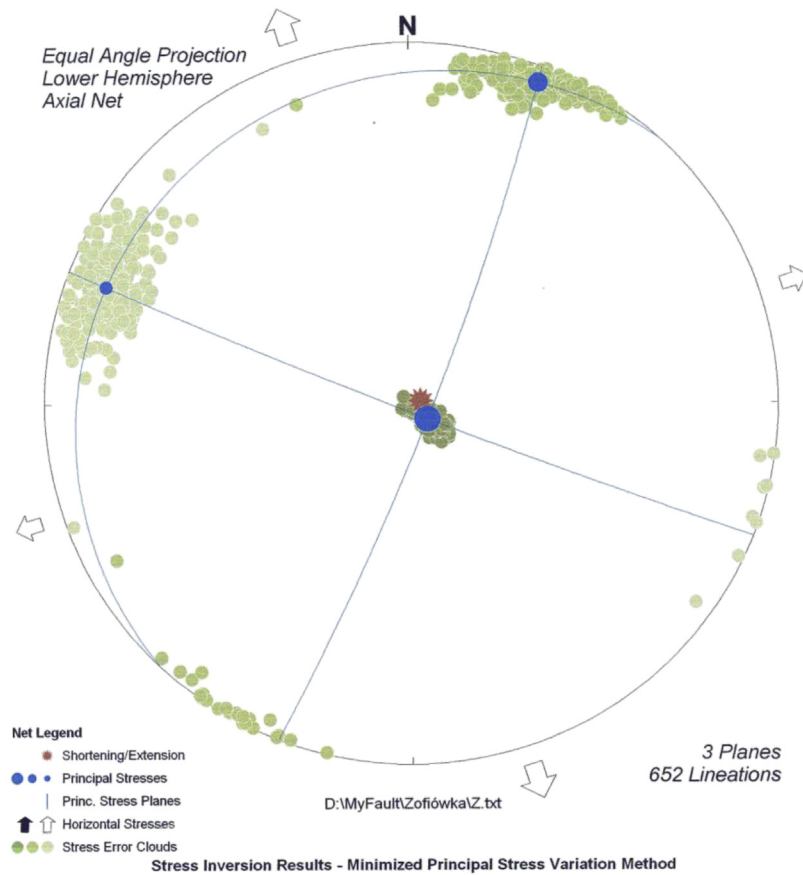


**Fig. 4 – System of stresses for a focus of tremor of normal fault type (there is dependence  $\sigma_1 > \sigma_2 > \sigma_3$ ).**



principal stresses. The data are a foundation to evaluate the stress state of the rock mass showing greater or lower tendency to generate high-energy tremors (Stec, 2012). It ought to be mentioned here that the spatial system of axes of principal stresses determines occurrence of a certain given type of tremor focal mechanism. Of course it is not possible to determine absolute values of stresses basing on seismological data. Yet, it is possible to determine their spatial location and mutual relations. The method basing on such data as parameters of focal mechanism tremors enables determining principal stresses assuming as follows: process of fracturing in the focus propagates along a specified plane and slip vector is parallel to shear stress in the plane. The calculation were made using MyFault software ([www.pangaearsci.com](http://www.pangaearsci.com)) based on the method Minimized Principal Stress Variation. This method, developed by Reches (1987), assumes that the stress

to cause fault slip obeys a Coulomb yield criterion,  $\tau = C + \mu\sigma$ , where  $\tau$  is the shear stress to cause slip,  $C$  is the cohesion stress,  $\mu$  is the friction coefficient and  $\sigma$  is the normal stress on the fault. From this relation, you can derive the principal stresses necessary for slip to occur. Assuming that all faults in the set were subject to the same regional stress state, then the principal stresses should be the same for all faults. Variations in material properties and other local effects will cause the actual stress state to vary between faults. To estimate the regional stress, we assume that the best value is found by minimizing the variations of the computed principal stresses within the fault set, using the same cohesion and friction coefficient for all faults. This assumption leads to a over determined set of linear equations in  $C$ ,  $\mu$  and six principal stress components.  $C$  is unknown and assumed to be zero because the mean stress (the so-called hydrostatic or



Principal stress $\sigma_1$ , (azimuth/plunge)	133°/83°
Principal stress $\sigma_2$ , (azimuth/plunge)	22°/3°
Principal stress $\sigma_3$ , (azimuth/plunge)	191°/7°
Stress ratio $R = (\sigma_2 - \sigma_3) / (\sigma_1 - \sigma_3)$ , $\sigma_1 \geq \sigma_2 \geq \sigma_3$	0.14
Misfit Angle $\pm$ error	16.7° $\pm$ 29,8°
Fault Angle $\pm$ error	38.2° $\pm$ 23.5°
Friction Angle	42.1°
Shear Stress	0.327 $\pm$ 0.028
Direction of Shortening/ Extension (azimuth/plunge)	74° / 87°

Fig. 5 – Results of calculations of parameters of stress distribution basing on slip focal mechanisms in the area of longwall H-2a.

lithostatic component), and hence the absolute normal stress, is unknown. All stresses are normalized such that the maximum principal stress  $\sigma_1$  is 1.0 and the minimum  $\sigma_2$  is 0.0. Thus, the stress Ratio  $R = (\sigma_2 - \sigma_3)/(\sigma_1 - \sigma_3)$  is equal to the intermediate stress  $\sigma_2$ . To find the value of  $\mu$ , the friction coefficient, MyFault solves the equations using a range of friction angles from 0 to 45°, choosing the value that gives the minimum variation in principal stresses for all faults. In this method the uncertainties in these quantities are estimated using the bootstrap resampling method (Michael, 1987).

Basing on the above mentioned parameters it is possible to describe geomechanical conditions of the stress state in the rock mass in the areas of occurrence of tremor focuses.

Tremors of normal slip type focuses occur when vertical stress  $\sigma_1$  dominates. Scheme of creating such a type of a focus is presented in Fig. 4.

Basing on tremors of normal shearing focal mechanism the mean local field of stresses was calculated for the area of longwall H-2a described with directions of axes of principal stresses  $\sigma_1$ ,  $\sigma_2$ ,  $\sigma_3$  (trend and plunge), stress Ratio  $R$  and other parameters shown below in Fig. 5.

The following system of stresses was obtained: principal stress  $\sigma_1$  was vertical (trend – 133°, plunge – 83°) and intermediate principal stress  $\sigma_2$  (trend – 22°, plunge – 3°) and minimal stress  $\sigma_3$  (trend – 291°, plunge – 7°) were horizontal. Stress ratio  $R$  was 0.14, which means dominating influence of stress  $\sigma_1$ . This type of state of stresses with dominating principal stress  $\sigma_1$  aimed vertically, characterises conditions which reflect the influence of the overlaying burden. Relative shear stress was 0.33 and the direction of its trend presented in Fig. 6 was roughly E–W. Horizontal stress marked in Figs. 5 and 6 with white arrows was a tensile one and its dominating direction of NW–SE was perpendicular to the gateroads. The Shortening/Extension axis, which is the direction of the biggest stress in a given area, was roughly vertical and was

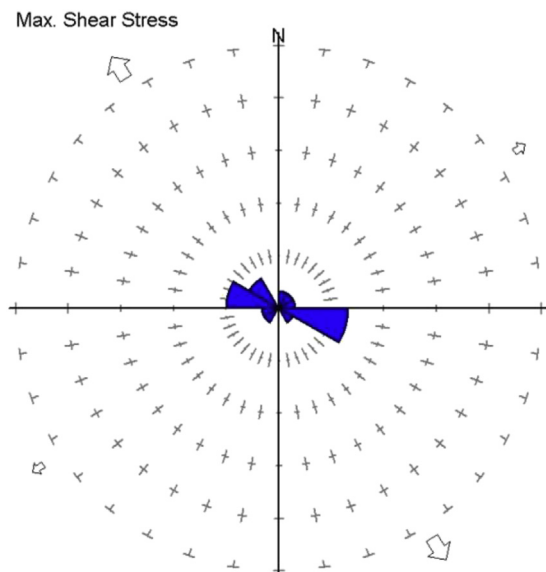


Fig. 6 – Trend of shear stress (blue) and direction of horizontal stress (white arrows) in the area of longwall H-2a.

located in a plane at approximately 45° angle towards the longwall face (trend – 74° and plunge – 87°).

## 5. Summary

The conducted research showed, that it is possible to obtain significant geomechanical data concerning assessment of seismic hazard basing on specialist interpretation of seismological data.

Basing on parameters of a focal mechanism and stress distribution  $\sigma_1$ ,  $\sigma_2$ ,  $\sigma_3$  expressed with their directions and relative values for the high-energy tremors which occurred while mining longwall H-2a of seam 409/3 in Borynia-Zofiówka-Jastrzębie Ruch Zofiówka colliery, stress state of the rock mass in the area was determined.

In the analysed area there was strong influence of fault structures surrounding the area of longwall H-2a, as directions of trend of nodal planes assumed as fracture planes in focuses are correlated with the direction of fault zones and a large share of shear processes in focuses of tremors.

Basing on the conducted research it can be concluded that the tremors were caused by displacement of roof layers over a selected goaf space, which gradually deflected and then dynamically fractured. An additional factor which significantly magnified the process was the influence of natural stresses existing in the rock mass, which originated from the fault zones surrounding the area of longwall H-2a.

## Source of financing

The research was conducted within the framework of research/service project titled “Determining processes in focuses of high energy tremors of energy of  $10^5$  J, occurring in lot H while mining seam 409/3, longwall H-2a, basing on their mechanisms” commissioned by Borynia-Zofiówka-Jastrzębie Ruch Zofiówka colliery Documentation no. 58107804-123.

## REFERENCES

- Bukowska, M. (2013). Post-peak failure modulus in problems of mining geo-mechanics. *Journal of Mining Science*, 49(5), 731–740. <http://dx.doi.org/10.1134/S1062739149050067>.
- Dokumentacja GIG nr 581 4793 3–141. (2013). *Prognoza zagrożenia sejsmicznego dla ściany H-2a w pokładzie 409/3 na dalszym jej wybiegu, po wystąpieniu wstrząsu o energii  $E = 4,6E6$  J w dniu 6.11.2013 r., który spowodował odprężenie w rejonie chodnika nadścianowego H-2, (niepublikowane)* [GIG Documentation no. 581 4793 3-141(2013) [Forecasting seismic hazard for further advance of longwall H-2a of seam 409/3 after a tremor of energy of  $E=4,6E6$  J of 6 November 2013, which caused destressing in the area of tailgate H-2, (unpublished)]]].
- Drzewiecki, J., & Kabiesz, J. (2008). Dynamic events in roof strata – occurrence and prevention. *Coal Science & Technology Magazine*, 55–57, 235, Huaihai Road (W) Xuzhou, Jiangsu, China, 221006.
- Drzewiecki, J., & Makówka, J. (2013). A model of rock mass fracturing ahead of the longwall face as a consequence of

- intensity of exploitation. *Acta Geodynamica et Geomaterialia*, 10(2), 137–145. <http://dx.doi.org/10.13168/AGG.2013.0013>.
- Dubiński, J. (2013). The mechanism and consequences of strong mining tremors that occur in Polish hard coal and copper mines. In *Proc. of EUROCK 2013-the 2013 ISRM International Symposium, Wrocław* (pp. 31–38). London, New York: Taylor & Francis Group, ISBN 978-1-138-00080-3.
- Dubiński, J., & Dworak, J. (1989). Recognition of the zones of seismic hazard in Polish coal mines by using a seismic method. *Pure and Applied Geophysics (PAGEOPH)*, 129(3), 171–178.
- FOCI software. Project Monitor. From <http://www.induced.pl>.
- Gibowicz, S. J., & Kijko, A. (1994). *Introduction to mining seismology* (p. 396). San Diego: Academic Press.
- Lurka, A. (1996). A certain new method for seismic network optimisation and its consequences. *Acta Montana A*, 10(102), 171–178.
- Lurka, A., & Logiewa, H. (2007). *Sejsmologiczny System Obserwacji SOS jako narzędzie do obserwacji i interpretacji danych sejsmicznych w górnictwie zagrożonym tąpnięciami* [SOS Seismological Observation System as a tool for observation and interpretation of seismic data in rockburst hazard mining] (pp. 283–296). Prace Naukowe Głównego Instytutu Górnictwa III/2007.
- Michael, A. J. (1987). Use of focal mechanisms to determine stress: a control study. *Journal of Geophysical Research: Solid Earth*, 92, 357–368.
- MyFault software. Project Monitor. Retrieved 2007 from <http://www.pangaeasci.com>.
- Reches, Z. (1987). Determination of the tectonic stress tensor from slip along faults that obey the Coulomb yield condition. *Tectonics*, 6(6), 849–861.
- Stec, K. (2012). Focal mechanisms of mine-induced seismic events an explanation of geomechanical processes in the area of longwall 6, seam 510 in hard coal mine Bobrek-Centrum. *Archives of Mining Sciences*, 57(4), 871–886. <http://dx.doi.org/10.2478/v10267-012-0057-7>.
- Stec, K., & Drzewiecki, J. (2012). Mine tremor focal mechanism: an essential element for recognizing the process of mine working destruction. *Acta Geophysica*, 60(2), 449–471. <http://dx.doi.org/10.2478/s11600-011-0036-y>.
- Wiejacz, P. (1991). *Investigation of focal mechanisms of mine tremors by the moment tensor inversion*. Ph.D. Thesis. Warsaw: Inst. Geophys. Pol. Acad. Sc (in Polish). (unpublished).